Hydrol. Earth Syst. Sci. Discuss., 10, 5975–6017, 2013
www.hydrol-earth-syst-sci-discuss.net/10/5975/2013/
doi:10.5194/hessd-10-5975-2013
© Author(s) 2013. CC Attribution 3.0 License.

Hydrology and Earth System Sciences
Open Access
Discussions

This discussion paper is/has been under review for the journal Hydrology and Earth System Sciences (HESS). Please refer to the corresponding final paper in HESS if available.

Assessment of statistical characteristics of point rainfall in the Onkaparinga catchment in South Australia

M. M. Rashid[1], **S. Beecham**[1], **and R. Chowdhury**[2]

[1]Centre for Water Management and Reuse, University of South Australia, Mawson Lakes, SA 5095, Australia
[2]Department of Civil and Environmental Engineering, United Arab Emirates University, Al Ain, P.O. Box 15551, UAE

Received: 5 April 2013 – Accepted: 23 April 2013 – Published: 14 May 2013

Correspondence to: M. M. Rashid (mdmamunur.rashid@mymail.unisa.edu.au)

Published by Copernicus Publications on behalf of the European Geosciences Union.

Abstract

Spatial and temporal variations in statistical characteristics of point rainfall are important for rainfall modelling. The main objective of this study was to investigate the statistical characteristics of point rainfall and to identify a probability distribution that can model the full spectrum of daily rainfall in the Onkaparinga catchment in South Australia. Daily rainfall data from 1960 to 2010 at thirteen rainfall stations were considered. Statistical moments and autocorrelation coefficients were estimated for rainfall depths at different temporal resolutions. The heterogeneity of monthly rainfall was tested using the Precipitation Concentration Index (PCI). Interannual variability of annual and seasonal PCI was observed. The catchment was characterized by unstable monthly rainfall with PCIs of more than 10 for all rainfall stations. Relatively strong and significant autocorrelation coefficients were observed for rainfall depths at finer (daily and monthly) temporal resolutions. The performance of different distribution models was examined considering their ability to regenerate various statistics such as standard deviation, skewness, frequency distribution, percentiles and extreme values. Model efficiency statistics of modelled percentiles of daily rainfall were found to be useful for optimum threshold selection in the hybrid distributions. A hybrid of the gamma and generalized pareto (GP) distributions was found to be more efficient than any single distribution (Weibull, gamma and exponential) for modelling the full range of daily rainfall across the catchment. In addition to this, a hybrid of the Weibull and GP distributions was also proposed. The outcomes from this study will assist water engineers and hydrologists to understand the spatial and temporal characteristics of point rainfall in the Onkaparinga catchment and will hopefully contribute to the improvement of rainfall modelling and downscaling techniques.

HESSD
10, 5975–6017, 2013

1 Introduction

Rainfall is one of the key inputs in hydrological modelling. The generation of rainfall, both temporally and spatially, is a relatively recent research topic in rainfall simulation and downscaling. The distribution of rainfall amounts over time and space can be an important input to decision making tools that provide information on rainfall variability and help in understanding the hydrological processes (Apaydin et al., 2006). Extreme rainfall has significant impacts on water resource management. According to the IPCC Fourth Assessment Report (AR4), extreme precipitation frequencies increased almost everywhere in the world over the 20th century and the trend will be continued into the 21st century (IPCC, 2007). Several studies have investigated temporal and spatial changes in extreme rainfall (Hennessy et al., 1999; Plummer et al., 1999; Suppiah and Hennessy, 1998). Plummer et al. (1999) and Hennessy et al. (1999) observed that heavy rainfall events and the number of rainy days both increased during the last century over Australia and that this increase depended on the season and region. Over the east and north portion of Australia, a significant increase in heavy rainfall has been observed in summer, while a decreasing trend was observed in south-west Western Australia (Hennessy et al., 1999). Suppiah and Hennessy (1998) observed an increasing trend in the 90th and 95th percentile rainfalls over most of Australia. Haylock and Nicholls (2000) reported a significant increase in total rainfall and number of rain days in the northern and southern regions of Australia.

Positively skewed probability distributions such as the Kappa, gamma, exponential, Weibull and mixed exponential are commonly used to model the frequency distribution of daily rainfall amount (Hanson and Vogel, 2008; Jamaludin and Jemain, 2007; Li et al., 2012b; Liu et al., 2011; SEN and Eljadid, 1999; Wan et al., 2005). These distributions are reasonably capable of reproducing low to moderate rainfall amounts but are generally not adequate for simulating rainfall extremes (Furrer and Katz, 2008; Wilks, 1999). Although simulation of extreme rainfall is a crucial challenge in rainfall modelling, only a limited number of studies have been undertaken. Wilks (1999) reported

HESSD
10, 5975–6017, 2013

that the mixed exponential distribution reproduced extreme rainfall (in case of rainfall less than 100 mm) better than the gamma distribution. A few researchers have used parametric compound distributions in order to simulate the full range of rainfall (Furrer and Katz, 2008; Hundecha et al., 2009; Vrac and Naveau, 2007), but these were generally criticised because of limitations such as numerical instability, data sensitivity and computational demand. The non-parametric approach where rainfall is modelled by resampling of the observed historical rainfall has been used by Lall and Sharma (1996) and Rajagopalan and Lall (1999). This approach generally leads to underestimation of extreme rainfall events (Markovich, 2007). A hybrid of the gamma and exponential distributions along with the generalized pareto (GP) distribution were implemented by Furrer and Katz (2008) and Li et al. (2012a) respectively, in order to simulate the entire range of daily rainfall. They found that hybrid distributions can be a substantial improvement over gamma or exponential distributions for simulating extreme rainfall.

Assessment of the capability of statistical distributions to simulate various temporal and extreme characteristics of rainfall is necessary before using such distributions in a rainfall generator or downscaling model. The performance of a probability distribution can vary temporally. Wan et al. (2005) observed that the mixed exponential distribution performs well in the summer season, whereas the gamma distribution is suitable for the winter season in Canada. Li et al. (2012b) fitted six probability distributions to daily rainfall from 24 stations in Canada and assessed their performance based on their ability to reproduce several key statistics such as mean, standard deviation and percentiles of daily, monthly and annual rainfall. They observed that the performance of reproducing key statistics of rainfall time series is proportional to the number of parameters in the distribution function. They also identified that the three-parameter (mixed exponential) distribution outperformed others in simulation of rainfall amounts. The distribution of rainfall amounts in different months and seasons is also important for water resources planning and management. The Precipitation Concentration Index (PCI) (Oliver, 1980) is a widely used index that has been applied for this purpose by various researchers (Apaydin et al., 2006; De Luis et al., 2010, 2011; Michiels et al., 1992; Ngongondo

HESSD
10, 5975–6017, 2013

et al., 2011). Higher values of PCI indicate a higher concentration of rainfall and vice versa. Ngongondo et al. (2011) found an unstable monthly rainfall regime in Malawi, with PCI values of more than 10. De Luis et al. (2011) studied the mean values of annual, seasonal, wet and dry periods of PCI in Spain. They found a significant change in PCI between two periods (1946–1975 and 1976–2005).

In this study, firstly we have fitted three widely used single probability distributions (gamma, exponential and Weibull) to assess their limitations in modelling rainfall extremes. Secondly, we have used a hybrid of the gamma and generalised Pareto (GP) distributions (Furrer and Katz, 2008) to model the full spectrum of daily rainfall in the Onkaparinga catchment in South Australia. Various statistics such as standard deviation, skewness, frequency distribution, percentiles and extreme values of observed and modelled rainfall were used to quantify the performance of the hybrid model. In addition, model efficiency statistics such as the coefficient of efficiency and the index of agreement were also used. Moreover, we have discussed how an efficient threshold can be selected in the hybrid modelling approach by examining various percentiles of observed and modelled rainfall. Finally, a hybrid of the Weibull and GP distributions is proposed in this study for modelling daily rainfall frequency distributions in the Onkaparinga catchment. We have also characterized the annual and seasonal rainfall concentrations in the Onkaparinga catchment using PCI.

2 Study area and data

Daily rainfall time series were provided by the Bureau of Meteorology, Australia. Thirteen rainfall stations were selected which are spread across the Onkaparinga catchment, as shown in Fig. 1. The details of the selected rainfall stations are listed in Table 1. Daily rainfall data for the period 1960 to 2010 were used for this study. These rainfall stations were previously used by Teoh (2003) who found that the temporal homogeneity of rainfall data at these stations was satisfactory. Seven of these selected stations match with the stations selected by Heneker and Cresswell (2010), who used

HESSD
10, 5975–6017, 2013

a network of 20 stations for the assessment of potential climate change impact on the water resources across the Mount Lofty Ranges. The catchment is approximately 25 km southeast of the city of Adelaide in South Australia. About 60 % of Adelaide's municipal water is supplied from the Onkaparinga catchment. The median annual rainfall over the area is approximately 770 mm but this varies with a strong gradient from approximately 400 mm near the coast to 1170 mm in upstream areas (Teoh, 2003). The catchment has a strong seasonal rainfall variation with less rainfall in summer (December–February) and higher rainfall during winter (June–August) (Beecham et al., 2013).

3 Methodology

3.1 Statistical moments and autocorrelation

For any time series x_t (where x_1, x_2,..., x_n are the rainfall depths at a uniform time interval t) with a sample size n, the various statistical moments used in this study such as mean ($\overline{x}$), standard deviation (s), skewness (g) and kurtosis (k) are defined by Eqs. (1), (2), (3) and (4), respectively (Sheskin, 2004).

$$\overline{x} = \frac{\sum_{t=1}^{n} x_t}{n} \quad (1)$$

$$s = \sqrt{\frac{\sum_{t=1}^{n} \left(x_t - \overline{x}\right)^2}{n-1}} \quad (2)$$

$$g = \frac{n \sum_{t=1}^{n} \left(x_t - \overline{x}\right)^3}{[(n-1)(n-2)]s^3} \quad (3)$$

HESSD
10, 5975–6017, 2013

$$k = \frac{n(n+1)(n-1)^2}{(n-1)(n-2)(n-3)} \left[\frac{\sum_{t=1}^{n} \left(x_t - \overline{x}\right)^4}{\left\{ \sum_{t=1}^{n} \left(x_t - \overline{x}\right) \right\}^2} \right] - 3\frac{(n-1)^2}{(n-2)(n-3)} \quad (4)$$

Rainfall data may exhibit serial correlation as the data are collected over time. This can be checked by estimating the autocorrelation function (ACF) for the time series. The autocorrelation function is a measure of correlation between two values x_t and x_{t+k} for a lag k, which can be defined as (Box et al., 2011; Khan et al., 2006):

$$R = \frac{\frac{1}{n} \sum_{t=1}^{n-k} \left(x_t - \overline{x}\right)\left(x_{t+k} - \overline{x}\right)}{\frac{1}{1-n} \sum_{t=1}^{n} \left(x_t - \overline{x}\right)^2} \quad (5)$$

$$\left(-1 - 1.645\sqrt{n-2}\right)/(n-1) \le R \le \left(-1 + 1.645\sqrt{n-2}\right)/(n-1) \quad (6)$$

where R is the ACF for any lag k and $\overline{x}$ is the mean of the time series. If the value of R for any lag lies outside the interval defined by Eq. (6), then the time series has significant serial correlation at that lag at the 95 % confidence limit. If the lag 1 ACF is outside of this interval, it is assumed that the time series is not composed of random observations.

3.2 Probability distribution model

One parameter (exponential), two parameter (gamma and Weibull) and three parameter (hybrid gamma and GP) distributions is used in this study to model the frequency distribution of daily rainfall. The generalized extreme value (GEV) distribution is used for frequency analysis. The probability density function and corresponding parameters of different single distributions used in this study are listed in Table 2.

HESSD
10, 5975–6017, 2013

The hybrid gamma and GP distribution (termed as hybrid distribution hereafter) proposed by Furrer and Katz (2008) has been applied in this study. In this hybrid model, rainfall depth is estimated by a gamma distribution which, when higher than a threshold value, is replaced by the GP distribution. The probability density function of the hybrid distribution is defined as:

$$h(x) = f(x;a,b)I(x \le u) + [1 - F(u;a,b)]g(x;k,\sigma,u)I(x > u) \quad (7)$$

where f and F are the density and cumulative distribution functions of the gamma distribution. The density function of the GP distribution over a threshold u is denoted by g with shape and scale parameters k and σ, respectively. I is the indicator function and $[1 - F(u;a,b)]$ is the normalization factor. In order to make the hybrid density function continuous at the junction of two distributions i.e. threshold (u), it is necessary that $h(u-) = h(u+)$. The shape parameter of the GP distribution is obtained from the GP distribution fitted to the rainfall data above the threshold value and is directly used in the hybrid distribution whereas the scale parameter can be estimated as:

$$\sigma = \frac{1 - F(u;a,b)}{f(u;a,b)} \quad (8)$$

In this research, we have used the maximum likelihood estimators (MLEs) to estimate the parameters of the different distributions. The method of moments is an alternative to MLE but can be a poor estimator due to its inefficiency to estimate small values of the shape parameter (Thom, 1958; Wilks, 1990, 1995). In the case of the hybrid distribution, application of MLE directly to estimate the parameter is difficult. Instead, we have followed the procedure suggested by Furrer and Katz (2008). First the scale and shape parameters of the gamma distribution were estimated by the MLE method considering the entire rainfall series. After selecting a suitable threshold value (u), GP distribution parameters were estimated by MLE from rainfall data above u. Finally, the scale parameter of the GP distribution was adjusted to obtain a continuous density.

HESSD
10, 5975–6017, 2013

3.3 Goodness of fit statistic

The two sample Kolmogorov–Smirnov test (KS-test) is a non parametric hypothesis test to check the null hypothesis that the data follow a specified distribution. We have used the KS-statistics in this study as a measure of the best fit distribution which is defined as the largest absolute difference between the theoretical and empirical cumulative distribution functions. Mathematically, this is expressed as:

$$\text{KS-statistics} = \max_{i=1}^{N} |F(X_i) - F(Y_i)| \tag{9}$$

where $F(X_i)$ and $F(Y_i)$ are the empirical and theoretical cumulative distribution functions for a sample size N.

The mean absolute error (MAE) of a cumulative distribution function (cdf) represents the mean of the absolute difference between the theoretical and empirical cdfs, and can also be used to examine how well a theoretical distribution is fitted to random data. The MAE-cdf is given by:

$$\text{MAE-cdf} = \frac{\sum_{i=1}^{N} |F(x_i) - F(Y_i)|}{N} \tag{10}$$

The modified coefficient of efficiency (E) and the index of agreement (d) statistics have been used in this study, as described by Eqs. (11) and (12), where O_i, P_i and $\overline{O}$ are the observed data, model simulated data and observed mean, respectively (Krause et al., 2005; Legates and McCabe Jr., 1999). The range of values for E varies from 1.0 (perfect fit) to $-\infty$ and a value less than zero indicates that the mean of the observed series would be a better predictor than the model. The index of agreement (d) varies

HESSD
10, 5975–6017, 2013

between 0 (no correlation) and 1 (perfect fit).

$$E = 1.0 - \frac{\sum_{i=1}^{N} |O_i - P_i|}{\sum_{i=1}^{N} \left|O_i - \overline{O}\right|} \tag{11}$$

$$d = 1.0 - \frac{\sum_{i=1}^{N} |O_i - P_i|}{\sum_{i=1}^{N} \left(\left|P_i - \overline{O}\right| + \left|O_i - \overline{O}\right|\right)} \tag{12}$$

The quantile ($Q - Q$) plot, which is applied in this study, is a useful graphical method to compare the probability distributions of two series of data. If the observed and simulated series have identical distributions, then the plotting of their quantiles will be a straight line with a slope of 1 : 1, pointed through the origin (Wilk and Gnanadesikan, 1968).

3.4 Precipitation Concentration Index (PCI)

Rainfall heterogeneity over a period of time can be investigated by PCI. The PCI of annual and seasonal rainfall can be calculated by Eqs. (13) and (14), which were intro-

HESSD
10, 5975–6017, 2013

duced by Oliver (1980) and further modified by De Luis et al. (2000).

$$\mathrm{PCI}_{\mathrm{annual}} = 100 \cdot \frac{\sum_{i=1}^{12} P_i^2}{\left(\sum_{i=1}^{12} P_i\right)^2} \tag{13}$$

$$\mathrm{PCI}_{\mathrm{seasonal}} = 25 \cdot \frac{\sum_{i=1}^{3} P_i^2}{\left(\sum_{i=1}^{3} P_i\right)^2} \tag{14}$$

where P_i is the monthly rainfall (mm) in any month i. For seasonal PCI, the Australian seasons are considered as summer (December–February), autumn (March–May), winter (June–August) and spring (September–November). PCI values less than 10 indicate a uniform rainfall distribution; values between 11 and 15 denote a moderate rainfall distribution; values from 16 to 20 suggest an irregular distribution; and values above 20 represent a strong irregularity in precipitation concentration (De Luis et al., 2011; Oliver, 1980).

3.5 Daily rainfall generation

As this study is investigating rainfall amounts, only daily rainfall depth was modelled for the observed wet days. The parameters for each probability distribution for each station were estimated by the MLE method. Estimated parameters were used as inputs in the probability distribution model to generate daily rainfall time series for each individual rainfall station over the period 1960 to 2010.

HESSD
10, 5975–6017, 2013

4 Results and discussion

Statistical moments and lag 1 autocorrelation coefficients of rainfall for different temporal resolutions are listed in Table 3. Both spatial and temporal variation was observed in the statistical moments. Rainfall series for all temporal resolutions (except annual) had positive skewness, which indicates a right skewed distribution. A high right skewed distribution was observed for the finest temporal resolution (day) and this reduced as the temporal resolution increased from day to annual. A negative skewness was found in a few stations for the annual rainfall series. In the case of kurtosis, relatively high values were observed for daily rainfall and low values were observed for monthly, seasonal and annual rainfall series. On the whole, the rainfall series at a fine resolution (day) display a strong right skewed distribution with a sharp peak near the mean whereas rainfall series at coarse resolutions (month, season, annual) have less skewed distributions with relatively flat peaks. Significant lag 1 autocorrelation (lag 1 ACF) was observed at all rainfall stations for daily and monthly rainfalls. In summer (DJF), a significant lag 1 autocorrelation was observed at four stations whereas no stations showed any significant lag 1 ACF for other seasons. For annual rainfall, three stations showed significant (at the 5 % level) lag 1 ACF and six stations showed lag 1 ACF significant at the 10 % level.

4.1 Probability distribution

4.1.1 Single distribution

In this study, commonly used probability distributions such as exponential, gamma and Weibull have been fitted to the daily rainfall for thirteen rainfall stations. Table 4 lists the summary of goodness of fit statistics, including KS-statistics and MAE. It was observed that the gamma and Weibull had better capability to reproduce the empirical cumulative distribution of daily rainfall. The exponential distribution had less skill compared to the gamma and Weibull. However, all three distributions failed to simulate the high rainfall

HESSD
10, 5975–6017, 2013

depths, as shown in Fig. 2. The upper tails of the distribution were not heavy enough and continuously underestimated the extreme rainfall.

The scale and shape parameters obtained from the gamma distribution fitted to daily non-zero rainfall from all thirteen rainfall stations were spatially interpolated using an Inverse Weighted Distance (IWD) technique to understand the spatial variability of rainfall through the study area, as shown in Fig. 3. The spatial distribution of gamma parameters in any area is a useful tool for understanding the spatial variability of rainfall. This was applied by Husak et al. (2006) for drought monitoring applications in Africa. Interpretation of the gamma distribution parameters is not straightforward unlike for single parameter distributions such as the normal distribution. Both the shape and scale parameter need to be interpreted together to acquire information from the gamma distribution. For example, areas with the same shape parameter values, but with different scale values, have different density functions.

It has been observed in this study that the area near the coast (downstream portion of the catchment) has a shape dominated rainfall pattern, which indicates that the area has a symmetrically distributed rainfall pattern with fewer extreme events. In contrast, the upstream (north–east) portion of the catchment shows a scale dominated rainfall region, which indicates more variability in the rainfall with more extreme events.

From Fig. 3, it is observed that the areas that experience a large amount of rainfall are described by large scale or small shape parameter values in the gamma distribution. The mean daily rainfall and mean number of wet days (> 0.5 mm) per year were spatially distributed, with these being lower in the downstream areas near the coast and higher in the upper catchment areas (Fig. 4).

4.1.2 Hybrid distribution

Application of the hybrid distribution (hybrid of gamma and generalized pareto distribution) improved the performance of the model for fitting the higher quantiles of the rainfall amounts, as shown in Fig. 5 (only rainfall stations G1, G3 and G7 are shown here).

HESSD
10, 5975–6017, 2013

Selection of an appropriate threshold in the hybrid distribution is crucial for its performance. The threshold should be neither too small nor too large (Li et al., 2012a). When different thresholds were applied to the hybrid distribution, it was observed that for comparatively lower thresholds, the higher quantiles of the observed rainfall series were overestimated, as shown in Fig. 5. The threshold is generally selected manually by trial and error. Quantile plots of observed and modelled rainfall can be used as a tool to identify a suitable threshold. Furrer and Katz (2008) recommended to choose a threshold in a region where the gamma distribution fits well.

Probability distributions were applied to observed rainfall at different stations and the daily rainfall was estimated. In the case of the hybrid distribution, a threshold value of 10 mm was selected for all stations. In order to further check the performance of each model in reproducing the observed rainfall, various percentiles of daily rainfall such as the 5th, 10th, 30th, 50th, 70th, 80th, 90th, 95th and 99th percentile values were estimated and plotted in Fig. 6 and this shows that single distributions (exponential, gamma and Weibull) are less skillful than the hybrid distribution to model higher percentile values of daily rainfall. For the lower percentiles (10th to 70th percentile) most of the models overestimated the observed rainfall whereas the hybrid model performed well for higher percentiles (90th percentile and above) of rainfall, as shown in Fig. 6. The goodness of fit statistics for different distribution models are given in Table 5. For the hybrid distribution, since rainfall amounts that are less than the threshold value (10 mm) have been modelled by the gamma distribution, there is no difference in the performance of the hybrid and gamma distributions for lower percentiles (less than 10 mm) as shown in Fig. 6 and Table 5. According to the efficiency statistics in Table 5, the Weibull distribution performed better than the gamma distribution in reproducing the lower percentiles of daily rainfall (below the threshold of the hybrid distribution) in all rainfall stations (only station G3 is shown here). Therefore, using a hybrid distribution consisting of the Weibull distribution for lower percentiles and the GP distribution for higher percentiles of daily rainfall will provide a better overall efficiency than the hybrid of the gamma and GP distributions for modelling the full spectrum of daily rainfall.

HESSD
10, 5975–6017, 2013

The quantile plot in Fig. 5 indicates that 10 mm is a suitable threshold for the hybrid model. This value, which is equal to the 68th percentile of daily rainfall, is used for the hybrid distribution at rainfall station G3. The scatter plot (Fig. 6) and goodness of fit statistics (Table 5) both show that the gamma distribution performed better than the hybrid distribution for the 50th, 70th and 80th percentiles of daily rainfall. Therefore a new threshold value of 25 mm, which is equal to the 90th percentile of daily rainfall, was selected and the new scatter plot (Fig. 7) and goodness of fit statistics (Table 6) show that the overall performance of the hybrid distribution has been improved. Selection of the threshold value for the hybrid model based on the quantile plots might be misleading. Therefore, the efficiency statistics and the scatter plot of the observed and modelled percentiles of rainfall have also been considered for optimum selection of the threshold value in the hybrid model.

Figure 8 shows the scatter plot of observed and simulated annual and seasonal rainfall totals and Table 7 shows the efficiency statistics. For annual and seasonal rainfall totals, the performance is more or less the same for all models except for the hybrid model. The model based on the Weibull distribution shows a slightly improved performance than the other distributions. The hybrid distribution exhibits a poorer performance compared to other single distributions (for example, the gamma) when simulated daily rainfall is aggregated to estimate the seasonal and yearly rainfall totals, which is an interesting finding. It is evident in Fig. 6 that the lower percentiles (for example, daily rainfall less than 15 mm for station G3) of daily rainfall are overestimated by the gamma distribution and even by the hybrid distribution. On the other hand, the higher percentiles of daily rainfall (daily rainfall greater than 15 mm for station G3) are under-predicted by the gamma distribution, which is counter balanced by the overestimation of the lower percentile rainfalls. In contrast, for the hybrid distribution, the overestimated lower percentile rainfalls are not counter-balanced by a noticeable underestimation of the higher percentile rainfalls. As a result, the annual total rainfall is always over-predicted by the hybrid distribution, more so than by a single distribution. From Table 8, it is clear that both the hybrid and gamma distributions overestimate the

HESSD
10, 5975–6017, 2013

total rainfall (below the threshold value of 15 mm) over the 51 yr period by 2572 mm. This is counterbalanced by the underestimated rainfall (1973 mm) above the threshold in the case of the gamma distribution, whereas the hybrid distribution is not able to counterbalance this, and instead again overestimates the rainfall above the threshold. Finally, considering the daily rainfall of station G3 over the period 1960 to 2010, the hybrid and the gamma distributions overestimated the 51 yr total rainfall by 2793 and 599 mm, respectively. This over-prediction varies from year to year due to the variability of the total amount of rainfall above and below the threshold. For example, for station G3 in the year 1960, the hybrid distribution over-predicted the annual total rainfall by 64.27 mm whereas the gamma distribution underestimated the annual total rainfall by 4.96 mm. In the following year (1961), annual rainfall is overestimated by 73.44 and 57.88 mm by the hybrid and gamma distributions, respectively. So the choice of rainfall distribution could be varied depending on the required temporal resolution (daily, monthly, seasonal and annual) of model output data. While the performance of the hybrid distribution for annual and seasonal rainfall simulation is not satisfactory compared to gamma and Weibull distributions, the hybrid distribution can reasonably reproduce the full range of observed daily rainfall in the Onkaparinga catchment.

This study shows that the hybrid distribution can satisfactorily reproduce the standard deviation and skewness of daily rainfall for all months as shown in Fig. 9.

A frequency analysis has been performed for rainfall extremes (99th percentile) of daily observed and modelled rainfall obtained for each year and each rainfall station by fitting the GEV distribution. Figure 10 shows the daily rainfall amounts for different average recurrence intervals (ARIs). The rainfall modelled by the hybrid distribution can reproduce the observed ARI rainfall more accurately compared to the values obtained by other distributions such as the gamma, exponential and Weibull. In the case of frequency analysis of annual total rainfall, the hybrid distribution shows less capability compared to the other single distributions (Fig. 11).

HESSD
10, 5975–6017, 2013

4.2 Precipitation concentration index (PCI)

PCI is a key index that provides information on the variability of rainfall over a period of time. For example, a lower PCI on an annual scale indicates that the rainfall total is uniform over each month of the year. PCI could therefore be a useful decision tool for sustainable water resources management. In this study, we have calculated the PCI for annual and seasonal scales. The spatial and interannual variation of PCI is shown in Fig. 12. The median values of annual and seasonal PCI were quite homogeneous throughout the study area. However, interannual variability was observed for both annual and seasonal PCI. Mean annual and seasonal (summer and autumn) PCI indicate a moderate precipitation concentration whereas winter and spring seasonal PCI values show a uniform precipitation concentration. The PCI analysis indicates that the period from December to May is more susceptible to extreme events than the period June to November. Interannual variability of PCI is found to be higher for seasonal and lower for annual temporal resolutions. Summer PCI shows the highest variability, while winter PCI exhibits the lowest variability as shown in the Fig. 13. This could be because the Adelaide region has winter dominant rainfall and the sparse nature of summer rainfall may lead to increased variability. Since the summer season exhibits moderate PCI values with high interannual variability, sustainable management of water resources in summer may be more challenging with increased vulnerability and reduced security of supply, which in turn may require more careful planning.

5 Conclusions

In this study, the limitation of applying widely used single distributions such as the gamma, exponential and Weibull to model the entire range (low to high) of daily rainfall time series has been demonstrated. Instead, a hybrid distribution of gamma and generalised pareto was fitted to observed daily rainfall data and this was found to reproduce the full spectrum of rainfall as demonstrated by several statistics including the

HESSD
10, 5975–6017, 2013

standard deviation, skewness, frequency distribution, percentiles and extreme values. The quantile plot, MAE of cdf and KS-statistics were used to identify the best fit probability distribution for daily rainfall.

The study shows that the gamma and Weibull distributions exhibit better performance in reproducing the rainfall compared to the exponential distribution. But none of these models reproduced the extreme rainfall depths satisfactorily. The spatial distribution of the shape and scale parameters of the gamma distribution provided important information on the characteristics of rainfall in the study area. Downstream regions near the coast of the Onkaparinga catchment displayed a shape dominant rainfall (less variability and fewer extreme events). In contrast, the upstream regions of the catchment were characterized by scale dominated rainfall (more variability and more extreme events).

Application of the hybrid gamma and GP distribution for daily rainfall modelling was able to reasonably model extreme events compared to the single distribution models. The quantile plots clearly indicate that the hybrid model is able to simulate the higher percentiles of daily rainfall well. The model can successfully reproduce the various percentiles of rainfall, standard deviation and skewness of monthly rainfall more so than other single distributions. However, the model performed less satisfactorily for annual and seasonal rainfall totals. The model performed well to reproduce the observed extreme rainfall (99th percentile) for different annual recurrence intervals for almost all rainfall stations.

Examining the model efficiency to simulate the observed percentiles of daily rainfall depth is useful for identifying an optimum threshold for a hybrid distribution. The study shows that the hybrid of the Weibull and GP distributions is reasonably better than the hybrid of the gamma and GP distributions, at least for the Onkaparinga catchment.

The median of the annual and seasonal PCIs was found to be approximately the same for all rainfall stations. However, interannual variability was observed in both the annual and seasonal PCIs. These values represent a moderate rainfall concentration in almost all stations throughout the year and for all seasons except winter. The summer PCI shows the highest variability whereas the winter PCI exhibits the lowest

HESSD
10, 5975–6017, 2013

variability. So it can be inferred that the sustainable management of water resources in the summer season is more challenging than in other seasons. This may help inform investment strategies.

Finally, it is expected that the incorporation of hybrid distributions in daily rainfall modelling and downscaling will improve the efficiency of models for simulating the entire range of daily rainfall time series. Moreover, the spatial distribution of the gamma parameters and variability of PCI will assist in developing more sustainable water resource management strategies.

Acknowledgements. This study was funded by the South Australian Government's Goyder Institute for Water Research through Grant C.1.1. The Goyder Institute also provided additional scholarship funding for the first author. The researchers are also grateful to the Australian Bureau of Meteorology for providing meteorological data.

References

Apaydin, H., Erpul, G., Bayramin, I., and Gabriels, D.: Evaluation of indices for characterizing the distribution and concentration of precipitation: a case for the region of Southeastern Anatolia Project, Turkey, J. Hydrol., 328, 726–732, 2006.

Beecham, S., Rashid, M. M., and Chowdhury, R.: Statistical downscaling of multi-site daily rainfall in a South Australian catchment using a generalized linear model, Int. J. Climatol., article under review, 2013.

Box, G. E., Jenkins, G. M., and Reinsel, G. C.: Time Series Analysis: Forecasting and Control, vol. 734, Wiley, New York, 2011.

De Luis, M., Raventós J., González-Hidalgo, J., Sánchez J., and Cortina, J.: Spatial analysis of rainfall trends in the region of Valencia (East Spain), Int. J. Climatol., 20, 1451–1469, 2000.

De Luis, M., González-Hidalgo, J., and Longares, L.: Is rainfall erosivity increasing in the Mediterranean Iberian Peninsula?, Land Degrad. Dev., 21, 139–144, 2010.

de Luis, M., González-Hidalgo, J. C., Brunetti, M., and Longares, L. A.: Precipitation concentration changes in Spain 1946–2005, Nat. Hazards Earth Syst. Sci., 11, 1259–1265, doi:10.5194/nhess-11-1259-2011, 2011.

HESSD

10, 5975–6017, 2013

Furrer, E. M. and Katz, R. W.: Improving the simulation of extreme precipitation events by stochastic weather generators, Water Resour. Res., 44, W12439, doi:10.1029/2008WR007316, 2008.
Hanson, L. S. and Vogel, R.: The probability distribution of daily rainfall in the United States, ASCEEWRI, World Environmental & Water Resource Congress, Honolulu, Hawaii, 12–16 May/American Society of Civil Engineers (ASCE), 2008.
Haylock, M. and Nicholls, N.: Trends in extreme rainfall indices for an updated high quality data set for Australia, 1910–1998, Int. J. Climatol., 20, 1533–1541, 2000.
Heneker, T. M. and Cresswell, D.: Potential impact on water resource availability in the Mount Lofty Ranges due to climate change, Technical report DFW 2010/03, Department of Water, for the Goverment of South Australia, Australia, 2010.
Hennessy, K. J., Suppiah, A., Forland, E., and Zhai, P.: Australian rainfall changes, 1910–1995, Austral. Meteorol. Mag., 48, 1–13, 1999.
Hundecha, Y., Pahlow, M., and Schumann, A.: Modeling of daily precipitation at multiple locations using a mixture of distributions to characterize the extremes, Water Resour. Res., 45, W12412, doi:10.1029/2008WR007453, 2009.
Husak, G. J., Michaelsen, J., and Funk, C.: Use of the gamma distribution to represent monthly rainfall in Africa for drought monitoring applications, Int. J. Climatol., 27, 935–944, 2006.
IPCC: Cliate Change 2007: The Physical Scienec Bias. Summary for Ploicymakers, onribution of Working Group I to the Fourth Assessmnt Report of the Intergivernmental Panel on Climate Change, IPCC Secretariat, Geneva, Switzerland, 2007.
Jamaludin, S. and Jemain, A. A.: Fitting daily rainfall amount in Malaysia using the normal transform distribution, J. Appl. Sci., 7, 1880–1886, 2007.
Khan, M. S., Coulibaly, P., and Dibike, Y.: Uncertainty analysis of statistical downscaling methods using Canadian Global Climate Model predictors, Hydrol. Process., 20, 3085–3104, 2006.
Krause, P., Boyle, D. P., and Bäse, F.: Comparison of different efficiency criteria for hydrological model assessment, Adv. Geosci., 5, 89–97, doi:10.5194/adgeo-5-89-2005, 2005.
Lall, U. and Sharma, A.: A nearest neighbor bootstrap for resampling hydrologic time series, Water Resour. Res., 32, 679–693, 1996.
Legates, D. R. and McCabe Jr., G. J.: Evaluating the use of "goodness-of-fit" measures in hydrologic and hydroclimatic model validation, Water Resour. Res., 35, 233–241, 1999.

HESSD
10, 5975–6017, 2013

Li, C., Singh, V. P., and Mishra, A. K.: Simulation of the entire range of daily precipitation using a hybrid probability distribution, Water Resour. Res., 48, W03521, doi:10.1029/2011WR011446, 2012a.
Li, Z., Brissette, F., and Chen, J.: Finding the most appropriate precipitation probability distribution for stochastic weather generation and hydrological modelling in Nordic watersheds, Hydrol. Process., doi:10.1002/hyp.9499, in press, 2012b.
Liu, Y., Zhang, W., Shao, Y., and Zhang, K.: A comparison of four precipitation distribution models used in daily stochastic models, Adv. Atmos. Sci., 28, 809–820, 2011.
Markovich, N.: Nonparametric Analysis of Univariate Heavy-Tailed Data: Research and Practice, John Wiley-Interscience, London, 806 pp., 2007.
Michiels, P., Gabriëls, D., and Hartmann, R.: Using the seasonal and temporal precipitation concentration index for characterizing the monthly rainfall distribution in Spain, Catena, 19, 43–58, 1992.
Ngongondo, C., Xu, C. Y., Gottschalk, L., and Alemaw, B.: Evaluation of spatial and temporal characteristics of rainfall in Malawi: a case of data scarce region, Theor. Appl. Climatol., 106, 79–93, 2011.
Oliver, J. E.: Monthly precipitation distribution: a comparative index, Prof. Geogr., 32, 300–309, 1980.
Plummer, N., Salinger, M. J., Nicholls, N., Suppiah, R., Hennessy, K. J., Leighton, R. M., Trewin, B., Page, C. M., and Lough, J. M.: Changes in climate extremes over the Australian region and New Zealand during the twentieth century, Clim. Change, 42, 183–202, 1999.
Rajagopalan, B. and Lall, U.: A k-nearest-neighbor simulator for daily precipitation and other weather variables, Water Resour. Res., 35, 3089–3101, 1999.
Sen, Z. and Eljadid, A. G.: Rainfall distribution function for Libya and rainfall prediction, Hydrol. Sci. J., 44, 665–680, 1999.
Sheskin, D.: Handbook of Parametric and Nonparametric Statistical Procedures, Second Edition, Chapman and Hall/CRC, Boca Raton, Florida, 2004.
Suppiah, R. and Hennessy, K. J.: Trend in total rainfall, heavy-rain events and number of dry days in Australia, 1910–1990, Int. J. Climatol., 10, 1141–1164, 1998.
Teoh, K. S.: Estimating the impact of current farm dams development on the surface water resources of the Onkaparinga River Catchment, DWLBC Report 2002/22, Department of Water, Land and Biodiversity Conservation, for the Government of South Australia, 2003.
Thom, H. C.: A note on gamma distribution, Mon. Weather Rev., 86, 117–122, 1958.

HESSD
10, 5975–6017, 2013

Vrac, M. and Naveau, P.: Stochastic downscaling of precipitation: From dry events to heavy rainfalls, Water Resour. Res., 43, W07402, doi:10.1029/2006WR005308, 2007.
Wan, H., Zhang, X., and Barrow, E. M.: Stochastic modelling of daily precipitation for Canada, Atmos. Ocean, 43, 23–32, 2005.
Wilk, M. B. and Gnanadesikan, R.: Probability plotting methods for the analysis for the analysis of data, Biometrika, 55, 1–17, 1968.
Wilks, D. S.: Maximum likelihood estimation for the gamma distribution using data containing zeros, J. Climate, 3, 1495–1501, 1990.
Wilks, D. S.: Statistical Methods in the Atmospheric Sciences: an Introduction, Academic Press, San Diego, CA, 1995.
Wilks, D. S.: Interannual variability and extreme-value characteristics of several stochastic daily precipitation models, Agr. Forest Meteorol., 93, 153–169, 1999.

HESSD
10, 5975–6017, 2013

Table 1. Details of selected rainfall stations used in the study.

BOM station ID	Station code	Latitude (decimal degree)	Longitude (decimal degree)	Elevation (m)	% missing (daily rainfall)
023726	G1	−34.9	138.87	459	15
023750	G2	−34.96	138.74	487	7.5
023707	G3	−35.01	138.76	445	14
023720	G4	−35.03	138.81	341	6.5
023709	G5	−35.06	138.66	376	0.41
023713	G6	−35.1	138.79	370	14.5
023710	G7	−35.11	138.62	267	10
023730	G8	−35.18	138.76	356	12
023753	G9	−35.27	138.56	104	11.6
023704	G10	−35.01	138.65	305	3.9
023721	G11	−35.06	138.56	170	0.22
023722	G12	−34.93	139.01	365	2.5
023733	G13	−35.06	138.85	363	0.41

HESSD
10, 5975–6017, 2013

Table 2. Probability distribution used in the study.

Name of the distribution	Probability density function	Parameters
Exponential	$f(x) = \frac{1}{\mu}\exp\left(-\frac{x}{\mu}\right), \quad x \geq 0, \quad \mu \geq 0$	x = daily rainfall amount μ = scale parameter
Gamma	$f(x) = \frac{b^{-a}x^{a-1}}{\Gamma(\alpha)}\exp\left(\frac{-x}{b}\right), \quad a > 0, \quad b > 0$	a = shape parameter b = scale parameter
Weibull	$f(x) = \frac{a}{b}\left(\frac{x}{b}\right)^{a-1}\exp\left[-\left(\frac{x}{b}\right)^{a}\right], \quad a > 0, \quad b > 0$	a = shape parameter b = scale parameter
Generalized Pareto (GP)	$f(x) = \frac{1}{\sigma}\left\{1 + \frac{\xi(x-u)}{\sigma}\right\}^{\left(-1-\frac{1}{\xi}\right)}, \quad x \geq u, \quad x \leq u - \left(\frac{\sigma}{\xi}\right)$	u = threshold σ = scale parameter ξ = shape parameter
Generalized extreme value (GEV)	$f(x) = \frac{1}{\sigma}\left[1 + \xi\left(\frac{x-\mu}{\sigma}\right)\right]^{\left(-1-\frac{1}{\xi}\right)}\exp\left\{-\left[1 + \xi\left(\frac{x-\mu}{\sigma}\right)\right]^{-\frac{1}{\xi}}\right\}$, $1 + \frac{\xi(x-\mu)}{\sigma} > 0$	μ = location parameter σ = scale parameter ξ = shape parameter

HESSD
10, 5975–6017, 2013

Table 3. Statistical moments and autocorrelation coefficients of rainfall at different temporal resolutions. DJF, MAM, JJA and SON represent summer (December to February), autumn (March to May), winter (June to August) and spring (September to November).

Rainfall temporal resolution	Statistical moments	Rainfall station												
		G1	G2	G3	G4	G5	G6	G7	G8	G9	G10	G11	G12	G13
Daily	Mean	2.69	3.05	2.98	2.31	2.47	2.32	2.32	2.49	1.88	2.37	1.83	1.59	2
	Std. dev.	7.73	7.99	8.06	6.03	5.96	6.41	5.98	6.64	5.28	6.29	4.78	4.67	5.32
	Skewness	5.45	4.72	4.81	4.91	4.3	5.54	4.77	5.11	5.41	4.58	5.12	6.41	5.75
	Kurtosis	49.247	33.985	33.89	38.51	28.67	53.44	36.84	41.7	51.95	30.44	40.91	70.57	60.83
	ACF(lag 1)	0.17[a]	0.22[a]	0.18[a]	0.26[a]	0.27[a]	0.14[a]	0.19[a]	0.17[a]	0.13[a]	0.2[a]	0.22[a]	0.24[a]	0.26[a]
Monthly	Mean	72.35	87.06	81.35	66.90	74.67	62.62	65.40	68.84	51.63	69.30	55.51	47.21	60.78
	Std. dev.	60.78	70.05	65.15	53.91	55.00	48.43	50.07	50.89	39.35	52.49	41.41	38.75	45.94
	Skewness	1.07	0.98	1.13	1.13	0.83	0.94	0.94	0.90	0.82	0.83	0.86	1.27	1.02
	Kurtosis	0.84	0.59	1.40	1.68	0.40	0.82	0.93	0.62	0.16	0.30	0.47	2.35	1.08
	ACF(lag 1)	0.45[a]	0.43[a]	0.46[a]	0.41[a]	0.44[a]	0.43[a]	0.43[a]	0.41[a]	0.44[a]	0.42[a]	0.41[a]	0.41[a]	0.37[a]
DJF	Mean	86.45	109.71	101.47	87.93	95.06	84.52	80.56	91.80	66.32	89.57	76.47	75.37	85.75
	Std. dev.	46.57	51.34	46.07	46.65	43.26	45.67	37.82	44.87	35.27	41.04	38.33	53.24	44.05
	Skewness	0.67	0.53	0.58	0.86	0.53	0.92	0.70	0.87	1.11	0.56	0.65	1.73	0.95
	Kurtosis	0.41	−0.28	−0.23	0.61	−0.14	0.53	0.07	0.75	2.26	0.29	−0.27	4.27	0.64
	ACF(lag 1)	0.19	0.27[a]	0.05	0.27[a]	0.23[b]	0.23[b]	0.19	0.19	0.18	0.13	0.14	−0.02	0.11
MAM	Mean	187.88	242.80	224.18	182.17	219.62	170.83	196.50	189.37	149.04	205.48	165.99	118.92	167.03
	Std. dev.	91.98	113.05	96.80	90.50	94.79	74.75	89.37	73.79	63.44	83.38	70.42	56.18	72.56
	Skewness	0.69	0.39	0.51	0.95	0.75	0.37	1.24	0.57	0.84	0.22	0.53	0.48	0.75
	Kurtosis	1.20	0.79	1.55	2.14	1.29	0.95	3.82	1.22	1.46	0.47	1.16	0.88	1.26
	ACF(lag 1)	0.01	−0.04	−0.07	0.06	−0.07	0.01	−0.10	−0.13	−0.16	−0.06	−0.07	−0.12	0.01
JJA	Mean	380.61	442.70	418.47	336.77	365.29	309.33	323.24	340.54	259.60	338.32	267.00	224.27	294.91
	Std. dev.	123.76	138.47	137.52	97.61	95.09	105.39	84.74	91.89	62.99	94.21	74.44	79.03	83.87
	Skewness	0.39	0.14	0.84	0.57	0.42	0.15	0.35	0.48	0.14	0.56	0.49	−0.21	0.33
	Kurtosis	0.55	0.55	1.32	1.00	0.26	1.90	0.40	0.73	−0.71	0.57	0.33	0.16	0.11
	ACF(lag 1)	−0.15	−0.05	0.14	−0.12	0.02	0.07	0.04	−0.10	−0.08	0.02	0.01	0.09	−0.12
SON	Mean	213.31	249.55	232.06	195.95	216.08	186.75	184.57	204.41	144.55	198.17	156.66	147.97	181.66
	Std. dev.	89.92	105.20	89.87	81.96	80.53	65.28	69.15	68.90	57.28	83.95	63.20	60.51	64.26
	Std. dev.	0.83	1.00	0.73	0.43	0.69	0.60	0.52	0.19	1.07	0.86	0.75	0.40	0.52
	Kurtosis	0.58	1.09	0.88	0.63	0.68	0.59	0.65	−0.07	1.43	0.73	0.53	0.75	0.53
	ACF(lag 1)	−0.15	−0.14	−0.11	−0.01	−0.06	−0.06	−0.03	−0.06	−0.11	−0.08	0.03	−0.19	−0.04
Annual	Mean	868.25	1044.75	976.19	802.82	896.05	751.42	784.86	826.11	619.50	831.55	666.11	566.53	729.35
	Std. dev.	221.70	238.48	202.15	191.39	170.00	171.94	165.60	145.86	124.86	163.12	138.94	158.63	149.22
	Skewness	−0.04	0.13	−0.13	0.16	0.17	−0.21	0.49	−0.29	0.56	−0.06	0.03	−0.37	0.20
	Kurtosis	1.43	1.79	0.08	0.41	0.33	0.42	0.20	0.10	0.62	0.05	−0.32	3.96	0.57
	ACF(lag 1)	−0.24[b]	−0.24[b]	−0.22[b]	−0.08	−0.22[b]	−0.24[b]	−0.12	−0.3[a]	−0.23[b]	−0.26[a]	−0.17	−0.14	−0.25[a]

[a] Significant at 0.05 level.
[b] Significant at 0.1 level.

HESSD
10, 5975–6017, 2013

Table 4. Summary of goodness of fit statistics for exponential, gamma and Weibull distributions fitted to daily non-zero rainfall.

	KS-statistics			MAE-cdf		
	Exponential	Gamma	Weibull	Exponential	Gamma	Weibull
Min	0.3793	0.0621	0.0719	0.0876	0.0217	0.0171
Mean	0.4189	0.0867	0.0831	0.1389	0.0285	0.0217
Max	0.4800	0.1239	0.1037	0.1820	0.0337	0.0264
Stad. Dev.	0.0291	0.0148	0.0099	0.0313	0.0043	0.0031

HESSD
10, 5975–6017, 2013

Table 5. Goodness of fit statistics for different percentiles of observed and modelled daily rainfall at station G3 (for hybrid distribution, the threshold is 10 mm).

Rainfall	Coefficient of efficiency (E)				Index of agreement (d)			
Percentile	Gamma	Exponential	Weibull	Hybrid	Gamma	Exponential	Weibull	Hybrid
5th	−0.48	−0.47	−0.87	−0.48	0.57	0.58	0.45	0.57
10th	0.39	−0.22	0.48	0.39	0.75	0.51	0.79	0.75
20th	0.07	−0.29	0.44	0.07	0.61	0.49	0.76	0.61
30th	−0.04	−0.29	0.28	−0.04	0.55	0.47	0.67	0.55
50th	0.18	0.07	0.39	0.11	0.60	0.56	0.69	0.58
70th	0.58	0.55	0.68	0.27	0.77	0.75	0.83	0.65
80th	0.81	0.78	0.86	0.84	0.90	0.88	0.92	0.91
90th	0.68	0.60	0.75	0.85	0.82	0.78	0.87	0.92
95th	0.44	0.33	0.59	0.87	0.70	0.65	0.78	0.93
99th	0.19	0.06	0.42	0.79	0.59	0.54	0.70	0.89

HESSD
10, 5975–6017, 2013

Table 6. Goodness of fit statistics for hybrid distribution with threshold 25 mm.

Rainfall	Coefficient of efficiency (E)				Index of agreement (d)			
Percentile	Gamma	Exponential	Weibull	Hybrid	Gamma	Exponential	Weibull	Hybrid
50th	0.18	0.07	0.39	0.18	0.60	0.56	0.69	0.60
70th	0.58	0.55	0.68	0.58	0.77	0.75	0.83	0.77
80th	0.81	0.78	0.86	0.84	0.90	0.88	0.92	0.91

HESSD
10, 5975–6017, 2013

Table 7. Goodness of fit statistics between observed and modelled rainfall for annual and seasonal rainfall.

Rainfall	Coefficient of efficiency (E)				Index of agreement (d)			
	Gamma	Exponential	Weibull	Hybrid	Gamma	Exponential	Weibull	Hybrid
Annual	0.81	0.77	0.87	0.69	0.90	0.88	0.93	0.85
DJF	0.82	0.79	0.88	0.83	0.91	0.89	0.94	0.91
MAM	0.83	0.81	0.88	0.85	0.91	0.90	0.94	0.93
JJA	0.85	0.83	0.90	0.83	0.92	0.91	0.95	0.91
SON	0.83	0.80	0.88	0.79	0.91	0.90	0.94	0.90

HESSD
10, 5975–6017, 2013

Table 8. Total rainfall over the period 1960–2010 below and above a 15 mm threshold for the hybrid and gamma distribution models for station G3.

Rainfall category	Total rainfall (mm)				
	Observed	Hybrid	Gamma	Observed-Hybrid	Observed-Gamma
≤ 15 mm	19 427	21 999	21 999	2572	2572
> 15 mm	30 012	30 233	28 039	221	−1973
			Total	2793	599

HESSD
10, 5975–6017, 2013

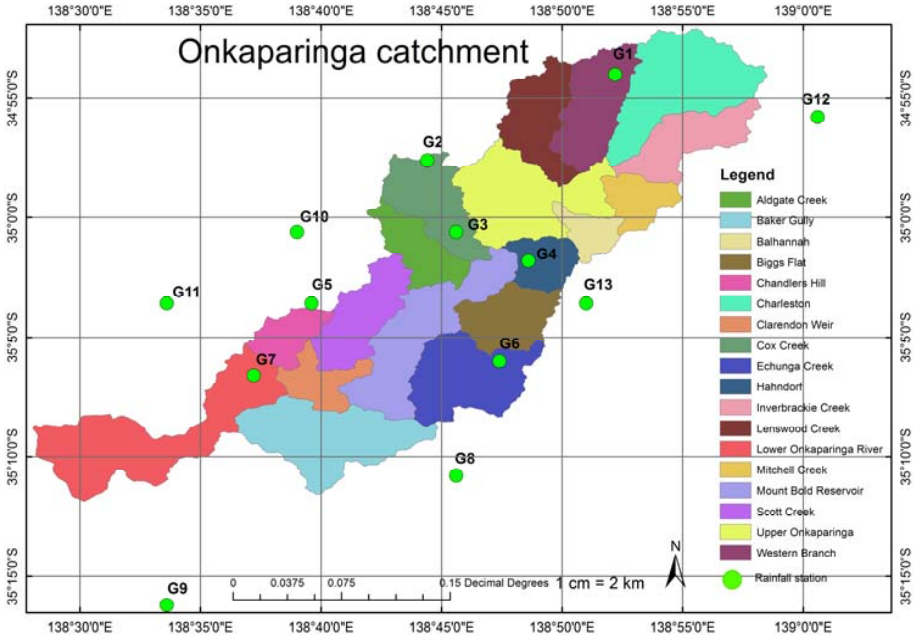

Fig. 1. The Onkaparinga catchment, it's sub-catchments and the location of rainfall stations.

HESSD
10, 5975–6017, 2013

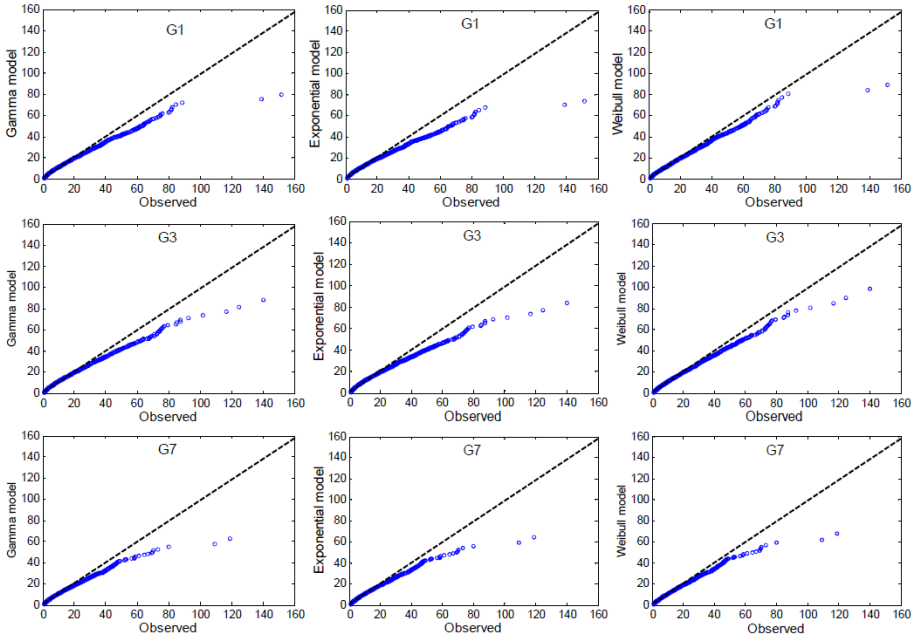

Fig. 2. QQ plots of observed versus gamma, exponential and Weibull modelled daily rainfall for stations G1 (top row), G3 (middle row) and G7 (bottom row).

HESSD
10, 5975–6017, 2013

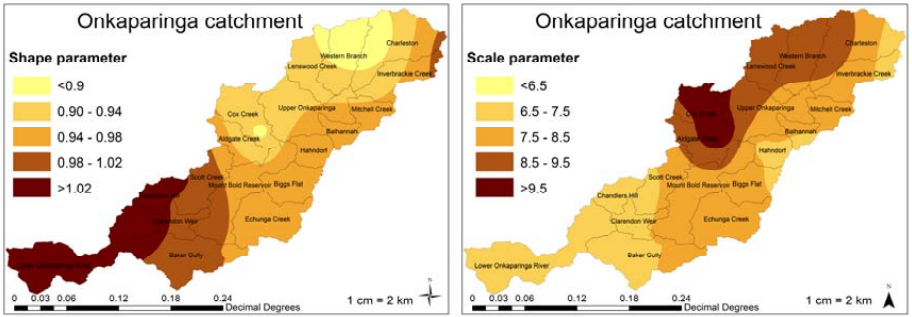

Fig. 3. Spatial distribution of shape and scale parameters of the gamma distribution.

HESSD
10, 5975–6017, 2013

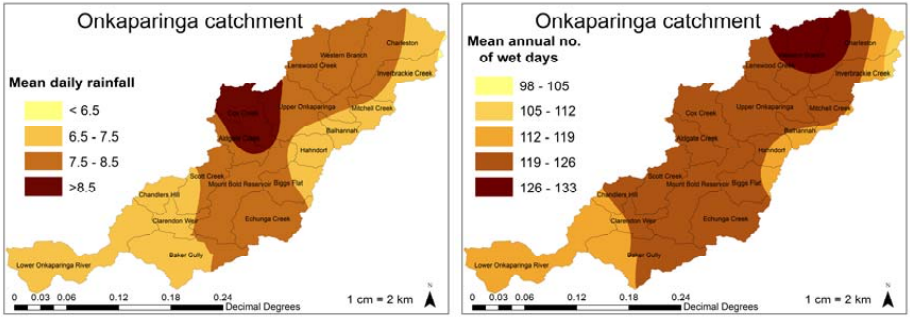

Fig. 4. Spatial distribution of mean daily rainfall and mean annual number of wet days.

HESSD
10, 5975–6017, 2013

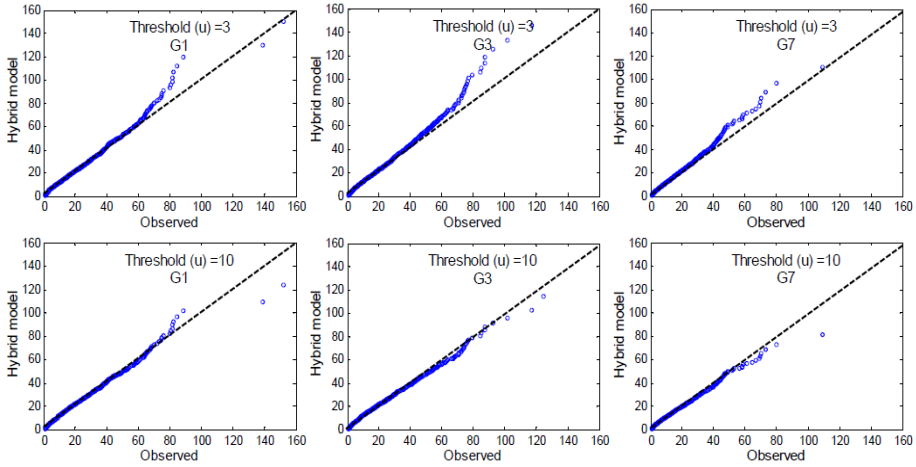

Fig. 5. QQ plot of observed versus hybrid modelled (HGP) daily rainfall for stations G1 (left), G3 (middle) and G7 (right) for different thresholds (top row = threshold of 3 mm and bottom row = threshold of 10 mm).

HESSD
10, 5975–6017, 2013

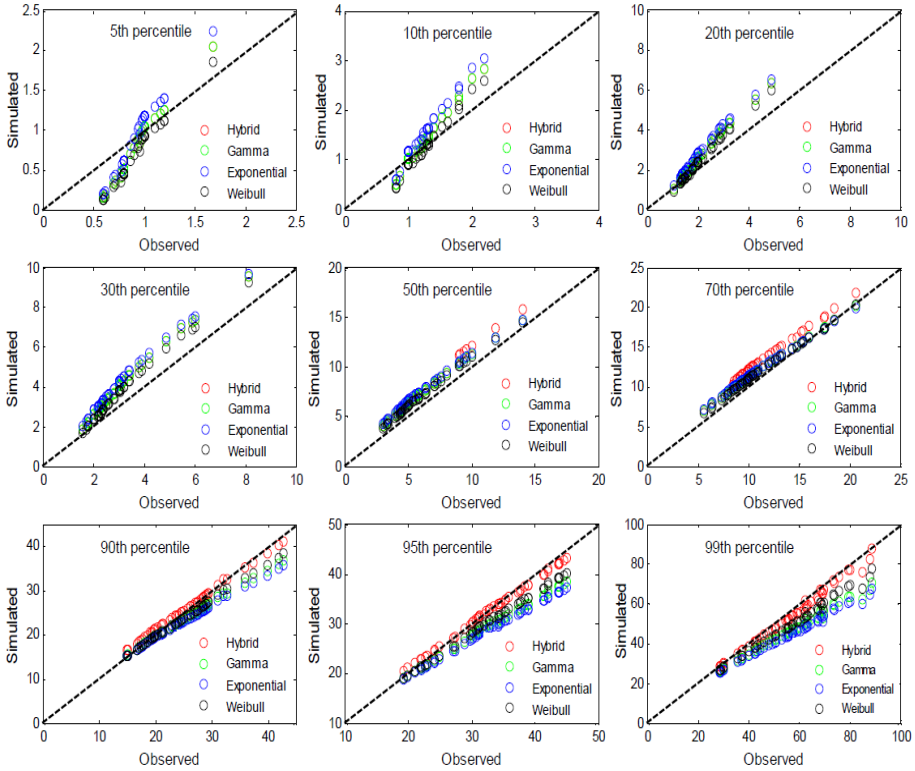

Fig. 6. Scatter plot of observed and modelled percentiles (5th, 10th, 20th, 30th, 50th, 70th, 90th, 95th, 99th) of daily precipitation at rainfall station G3. Dashed line represents the 1 : 1 reference line. Below the threshold legend of hybrid distribution is coincide with the legend of gamma distribution.

HESSD
10, 5975–6017, 2013

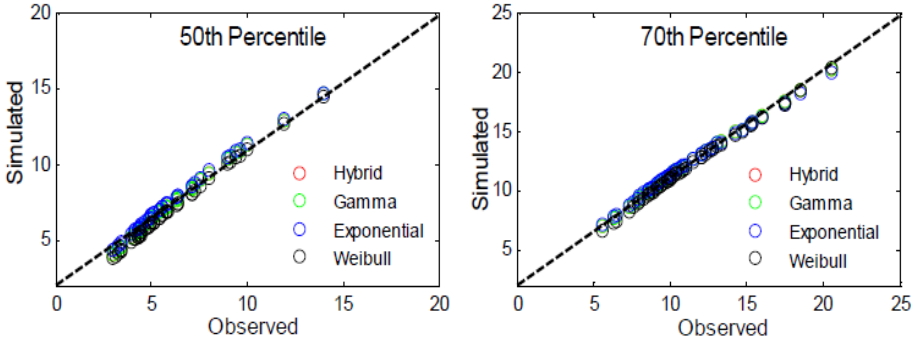

Fig. 7. Scatter plot of observed and modelled percentiles (50th and 70th) of daily precipitation at rainfall station G3 considering the threshold for the hybrid distribution as the 90th percentile of rainfall i.e. 25 mm. Dashed line represents the 1 : 1 reference line. Below the threshold legend of hybrid distribution is coincide with the legend of gamma distribution.

HESSD
10, 5975–6017, 2013

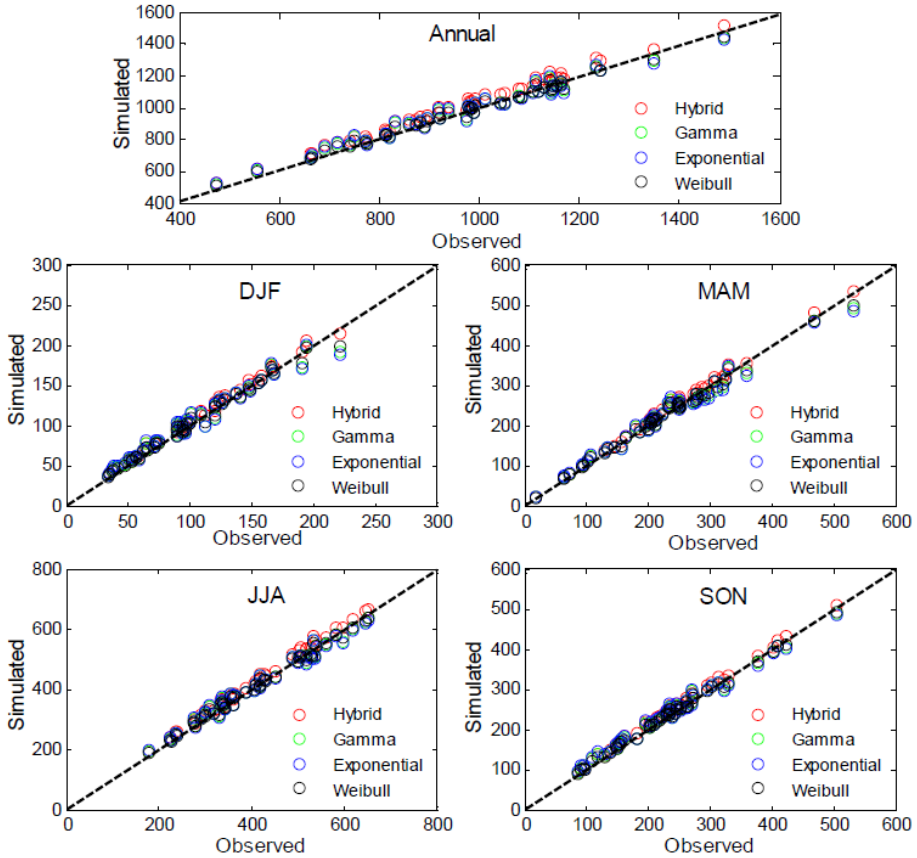

Fig. 8. Scatter plot of observed and modelled annual and seasonal rainfall at station G3 considering the threshold as the 90th percentile of rainfall i.e. 25 mm. Dashed line represents the 1 : 1 reference line.

HESSD
10, 5975–6017, 2013

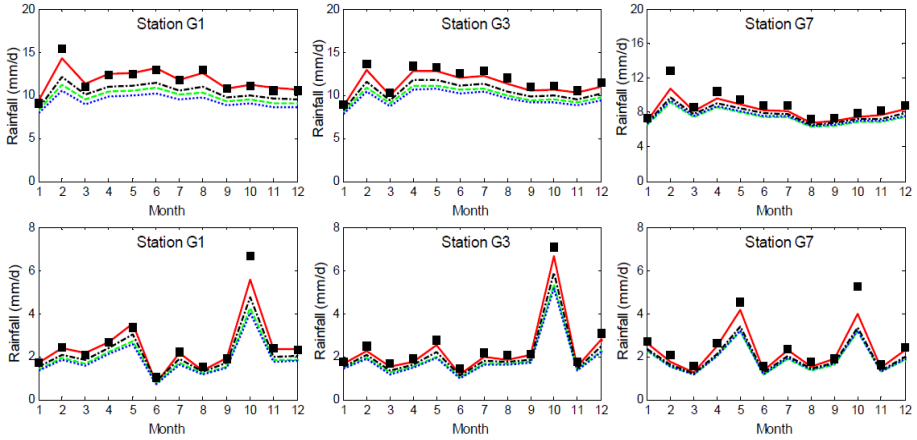

Fig. 9. Observed (solid square box) and modelled (red solid, green dashed, blue dotted and black dash-dot lines represent the model by hybrid, gamma, exponential and Weibull distributions, respectively) monthly standard deviation (top row) and skewness (bottom row) of daily rainfall.

HESSD
10, 5975–6017, 2013

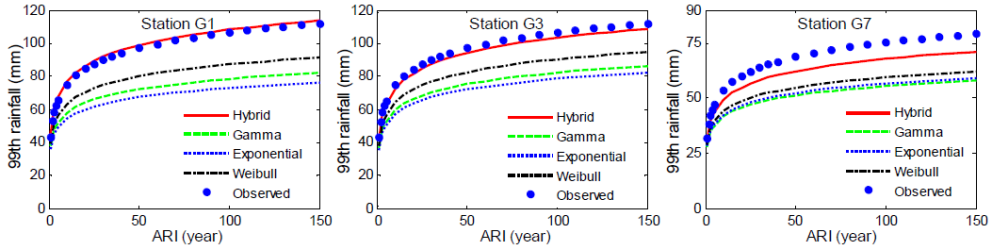

Fig. 10. Frequency distributions of observed and modelled 99th percentile of daily rainfall at stations G1, G3 and G7.

HESSD
10, 5975–6017, 2013

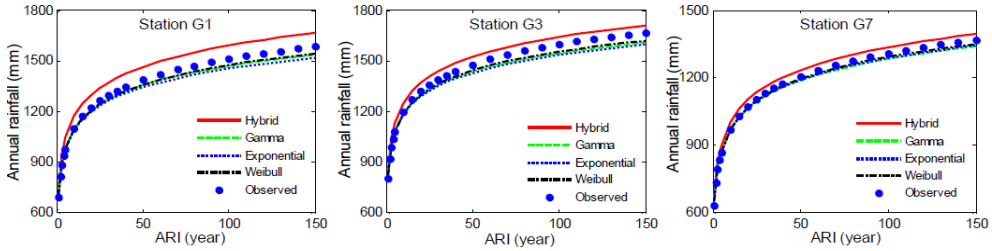

Fig. 11. Frequency distributions of observed and modelled annual total rainfall at stations G1, G3 and G7.

HESSD
10, 5975–6017, 2013

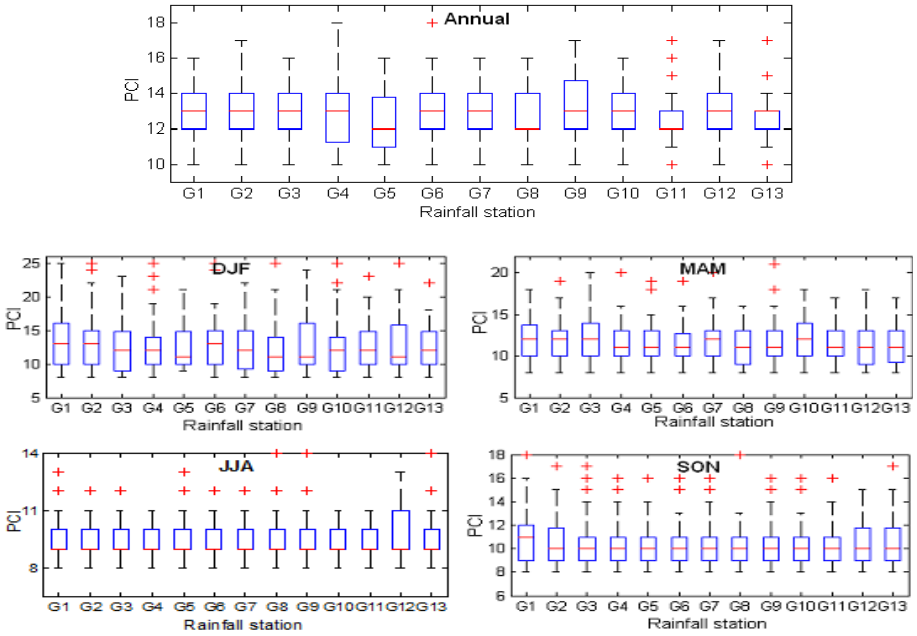

Fig. 12. Spatial and interannual variability of annual and seasonal PCI.

HESSD
10, 5975–6017, 2013

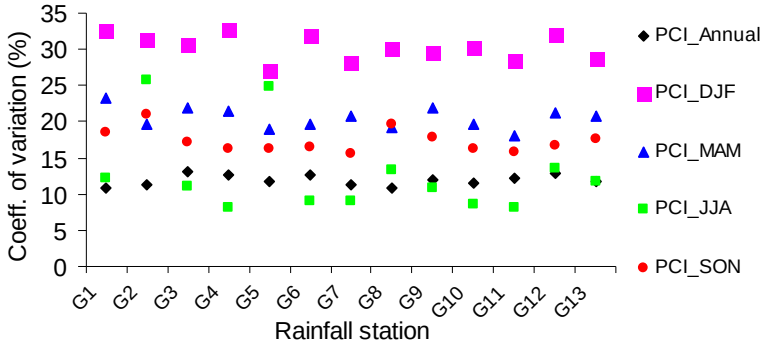

Fig. 13. Temporal variability of annual and seasonal PCI over the period 1960–2010 (DJF, MAM, JJA and SON are December-January-February, March-April-May, June-July-August, September-October-November, respectively.

HESSD
10, 5975–6017, 2013